

Peculiarities of hydroxyaryl oxidation by fungal peroxidase: reactivity and inhibition of the enzyme

J. Kulys*,

R. Vidziunaite,

A. Ziemys,

I. Bratkovskaja

Department of Enzyme Chemistry,
Institute of Biochemistry,
Mokslininkų 12, LT-08662 Vilnius,
Lithuania

The oxidation kinetics of hydroxyaryls (HAs), i. e. phenol, 1-naphthol, 2-naphthol, 4,4'-isopropylidene diphenol (bisphenol A), 4-hydroxybiphenyl and 1-hydroxypyrene, catalysed with the recombinant *Coprinus cinereus* peroxidase (rCiP) was investigated with an emphasis on the correlation between the structure and the function of the substrates.

The HAs showed different reactivity. The oxidation rate of HAs was maximal at pH 7.0–7.5. For 1-naphthol, an apparent pK_a of activity change was 5.6 and 9.4. The apparent bimolecular constant of HA oxidation (k_p) changed from $1.3 \cdot 10^5$ to $1.3 \cdot 10^8 \text{ M}^{-1}\text{s}^{-1}$ at pH 5.5 and 25 °C.

Comparison of the initial rate of HA oxidation with the calculated molecular parameters has shown that the rate-determining factors are the energy of molecular orbitals (redox potential) and the hydrophobicity of the substrates.

During exhaustive HA oxidation, peroxidase inhibition and microparticle formation were indicated. BSA and PEG prevented the inhibition and increased the oxidation yield of HA. A hypothesis was made that inhibition of rCiP is linked with formation of HA oligomer which bind in the active centre of peroxidase. The docking calculations show that these oligomers interact with the enzyme stronger than the substrates. The oligomers do not form productive complexes and block the active centre. BSA, PEG and other non-charged polymers that form a globular structure bind oligomers and prevent enzyme inhibition.

Key words: *Coprinus cinereus*, peroxidase, phenol, 1-naphthol, 2-naphthol, 4-hydroxybiphenyl, bisphenol A, 1-hydroxypyrene, BSA, PEG

INTRODUCTION

Phenol derivatives, i. e. hydroxyaryls (HAs), are a class of organic chemicals comprising many thousands of xenobiotics that are ubiquitous in the environment and in foodstuffs. They are produced and released into the environment by various industrial processes. Most of HAs are toxic and classified as pollutants dangerous for human and animal health [1]. Many of these compounds are highly resistant to biotic and abiotic degradation and, as a result, remain in the environment in contaminating levels. Enzyme-catalysed degradation of hydroxyaryls has been considered as one of the detoxification possibilities of these congeners [2–5]. Several oxidoreductases, e. g., peroxidases, laccase and bilirubin oxidase, catalyse the oxidative polymerisation of phenol derivatives [6–10].

The oxidation of peroxidases-catalysed phenol derivatives has several limitations, including permanent peroxidase inactivation by various undesirable side reactions [11–13]. In an attempt to decrease the inhibition rate, some additives were used [14–17]. It was shown that the oxidation yield of *Coprinus cinereus* peroxidase-catalysed phenol derivatives significantly increased if albumins or non-ionic polymeric compounds were used [17].

The goal of this work was to study the structure–function relation of HA reactivity with fungal peroxidase. The kinetics measurements were combined with quantum chemical *ab initio* and docking calculations. As hydroxyaryls, compounds containing single and multiple aryl residues, i. e. phenol, 4,4'-isopropylidenediphenol (bisphenol A), 4-hydroxybiphenyl, 1-naphthol, 2-naphthol and 1-hydroxypyrene, were investigated.

MATERIALS AND METHODS

Characteristics of peroxidase and materials

The recombinant peroxidase *Coprinus cinereus* (rCiP) was received from Novozymes A / S (Denmark). 4-hydroxybiphenyl, phenol, 30% perhydrol solution, sodium acetate, acetic acid, potassium hydrophosphate were obtained from Reachim (Russia). 1-naphthol and 2-naphthol were from Aldrich (USA), polyethylene glycol (PEG, MW 40,000) was from Ferak (Germany), 1-hydroxypyrene, 4,4'-isopropylidenediphenol (bisphenol A) and bovine serum albumin (BSA, 99%) were from Sigma (USA). The concentration of rCiP, hydrogen peroxide and BSA was determined spectrophotometrically. For rCiP, hydrogen peroxide and BSA, the extinction coefficients $\epsilon_{405} = 108 \text{ mM}^{-1} \cdot \text{cm}^{-1}$ [18], $\epsilon_{240} = 39.4 \text{ M}^{-1} \cdot \text{cm}^{-1}$ [19] and $\epsilon_{280} = 43.6 \text{ mM}^{-1} \cdot \text{cm}^{-1}$ [20] were used, respectively.

* Corresponding author. E-mail: jkulys@bchi.lt

Kinetic measurements

The kinetic measurements were performed at 25 ± 0.1 °C using a computer-controlled Ultrospec II LKB UV/Visible spectrophotometer and a computerized MPF-4 spectrofluorimeter (Hitachi, Japan). The fluorescence of 1- and 2-naphthol was measured at 460 nm and at excitation 320 nm and 328 nm, respectively. Respective parameters for 4-hydroxybiphenyl were 330 nm and 270 nm, for bisphenol A 310 nm and 280 nm, for 1-hydroxypyrene 410 nm and 350 nm, and for phenol 295 nm and 265 nm. The scattering of light was measured at 500 nm.

The measurements were performed in 50 mM acetate buffer (pH 4.5–6.0), 50 mM phosphate buffer (pH 6.0–8.5), 50 mM carbonate buffer (pH 8.5–10.5) at 25.0 ± 0.1 °C. The concentration of phenol was 11 μ M, bisphenol A 10 μ M, of naphthols 2.5–25 μ M, 4-hydroxybiphenyl 3–23 μ M and 1-hydroxypyrene 0.6–3 μ M. The concentration of hydrogen peroxide was 0.1 mM. The reaction was started by addition of rCiP. The fluorescence was calibrated using a fixed concentration of the substrates in the same buffer solution. The fluorescence intensity of the substrates was linearly proportional to their concentration only in a particular range, and the concentration of the substrates did not exceed 25 μ M for naphthols and for 4-hydroxybiphenyl.

The number of particles was determined by using a Hiac / Royco 9703 system of particle counting in liquids (USA). The 16-channel system was programmed for measuring the number of particles and their size distribution in the range 2.5–300 μ m.

The initial reaction rate (V_0) of 4-hydroxybiphenyl, 1-naphthol, 2-naphthol and 1-hydroxypyrene oxidation was determined by approximating the kinetic curves of fluorescence change with a linear function during 5–30 s. The V_0 was used for apparent V_{\max} and K_m calculations following the Michaelis–Menten kinetics. An apparent bimolecular constant (k_f) was calculated as $V_{\max} / K_m [E]_t$. The kinetic curves of bisphenol A and phenol fluorescence decrease were approximated with exponential decay, and the first-order constant (k_f) was calculated. The apparent bimolecular constant of these compounds was calculated as $k_f / [E]_t$.

Molecular calculations

The geometries and electronic structures of the substrates were calculated employing the Hartree–Fock theory using a 6–31G* basis set [21]. Atomic charges for docking calculations were calculated using *ab initio* calculations on a 3–21G basis set and the Hartree–Fock theory. The structure of *Arthromyces ramosus* peroxidase (ARP), which has one additional terminal amino group compared to *Coprinus cinereus* peroxidase is described [22]. The crystal data of ARP (PDB-ID: 1ARP) [22] with resolution of 1.9 Å were downloaded from the Protein Data Bank. All water molecules were removed, except the oxygen atom of one structural water molecule, which was left in the active centre of ARP. In order to model the catalytically active state of ARP, i. e. compound I / II, the distance of the Fe = O bond was set at 1.77 Å, i. e. the average Fe = O distance of compounds I and II of horseradish peroxidase [23].

Simulations of substrate docking in *Arthromyces ramosus* peroxidase (ARP) were performed with AutoDock 3.0.5 [24]. The electrostatic interaction energy grid used a distance-dependent dielectric Mehler–Solmajer function [25]. The docking

was accomplished using the Lamarckian genetic algorithm. The number of individuals in the populations was set at 50. The maximum number of energy evaluations that the genetic algorithm had to make was set at 1 000 000. Each docking was assigned to make 200 runs. Two sets of atomic interaction energy grid maps were calculated: the first one was prepared for dockings to the whole ARP surface (0.6 Å grid spacing, 126 grid points forming an about 75 Å cubic box centered on the geometric centre of the peroxidase) and the second one for docking in the active centre of ARP (0.375 Å grid spacing and 126 grid points forming about 75 Å cubic box centered at the geometric centre of the ARP active centre). The space of the cubic box of both sets covered the whole peroxidase with the space beyond and the active centre of ARP with the space beyond.

The polar surface area (PSA), total surface area (SA), distribution coefficient ($\log P$), lipole parameter were calculated with Vega [26]. The lipole is calculated as a sum of local values of $\log P$ for each atom as a dipolar momentum: summing all $r_i \cdot l_i$, where r_i is the distance between atom i and the geometric center of the molecule, l_i is the atomic value of the lipophilicity of atom i .

RESULTS AND DISCUSSION

Kinetics of hydroxyaryl oxidation

The oxidation of HA was performed in the presence of 0.037–30 nM rCiP. The initial rate of HA oxidation was directly proportional to rCiP concentration at 0.1 mM of hydrogen peroxide and 7–25 μ M of HAs. At 0.1 mM of hydrogen peroxide the dependence of initial rate on substrate concentration fitted Michaelis–Menten equation (Fig. 1). V_{\max} was 0.5 μ M/s, 2.0 μ M/s, 0.4 μ M/s, 0.03 μ M/s and K_m was 75 μ M, 175 μ M, 30 μ M, 6 μ M for 1-naphthol, 2-naphthol, 4-hydroxybiphenyl, 1-hydroxypyrene, respectively. The calculated apparent bimolecular constants covered a range $1.1 \cdot 10^7 - 1.3 \cdot 10^8 \text{ M}^{-1} \text{ s}^{-1}$ (Table 1). The apparent bimolecular constant of phenol was $1.3 \cdot 10^5 \text{ M}^{-1} \text{ s}^{-1}$ and was similar to that of bisphenol (Table 1).

A long-term fluorescence recording of 1-naphthol, 2-naphthol and 4-hydroxybiphenyl oxidation exposed saturation of the

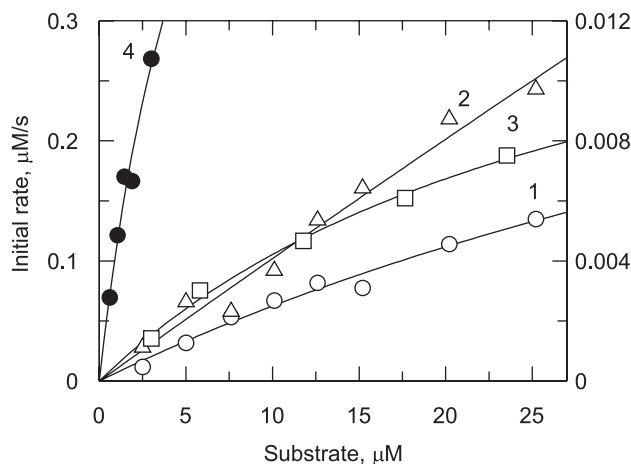


Fig. 1. Initial oxidation rate of 1-naphthol (1), 2-naphthol (2), 4-hydroxybiphenyl (3) and 1-hydroxypyrene (4) at pH 5.5. Curves 1–3 correspond to x - y axis; curve (4) corresponds to x - y second axis. Concentration of rCiP 0.51 nM (1, 2), 1.1 nM (3), 37 pM (4), 0.1 mM (1–4) of H_2O_2

Table 1. Constants of hydroxyaryl oxidation with rCiP, PEG action and light scattering during reaction at pH 5.5, 25 °C

Substrate	rCiP, nM	$k_p, M^{-1}s^{-1}$	PEG action	Light scattering
Phenol	30	$(1.3 \pm 0.1) \cdot 10^5$	No effect	Weak
Bisphenol A	95	$(1.3 \pm 0.2) \cdot 10^5$	No effect	Strong
4-hydroxybiphenyl	1.1	$(1.1 \pm 0.1) \cdot 10^7$	Strong	Strong
1-naphthol	0.5	$(1.4 \pm 0.1) \cdot 10^7$	Strong	Very strong
2-naphthol	0.5	$(2.3 \pm 0.2) \cdot 10^7$	Strong	Very strong
1-hydroxypyrene	0.037	$(1.3 \pm 0.2) \cdot 10^8$	No effect	Strong

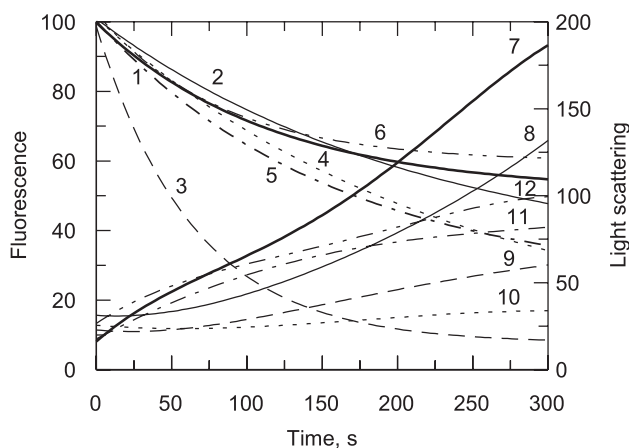


Fig. 2. Change of fluorescence (1–6) and light scattering (7–12) during HA oxidation. Concentration: 1-naphthol 25 μM (1, 7), 2-naphthol 25 μM (2, 8), 4-hydroxybiphenyl 10 μM (3, 9), phenol 11 μM (4, 10), 1-hydroxypyrene 7.3 μM (5, 11), bisphenol A 10 μM (6, 12), rCiP 0.5 nM (1, 2, 7, 8), 1 nM (3, 9), 40 nM (4, 10), 0.03 nM (5, 11), 57 nM (6, 12), H_2O_2 100 μM (1–12), 50 mM acetate buffer, pH 5.5, 25 °C

reaction rate (Fig. 2). This meant the enzyme inhibition during the reaction. The further addition of H_2O_2 did not affect the substrate oxidation rate, however, addition of a new portion of the enzyme increased the reaction rate. In contrast to these compounds, the oxidation of phenol and 1-hydroxypyrene followed almost completely the first-order reaction without peroxidase inhibition.

Addition into the reaction mixture of BSA or PEG increased the rate of 1-naphthol (Fig. 3) as well as 2-naphthol and 4-hydroxybiphenyl oxidation. Almost all 1-naphthol was oxidized in presence of 200 nM of BSA or 20 nM of PEG. This meant that BSA and PEG prevented peroxidase inhibition during naphthol oxidation.

During oxidation of HAs, an increased solution light scattering was observed (Figs. 2, 3). The increase of light scattering was largest for 1- and 2-naphthols. A lower effect was observed during bisphenol A, 1-hydroxypyrene and phenol oxidation. The light scattering practically didn't change during 4-hydroxybiphenyl oxidation. Comparison of HA oxidation and light scattering showed that a larger scattering followed a better peroxidase inhibition.

The addition of BSA and PEG changed light scattering kinetics during 1-naphthol oxidation (Fig. 3). The intensity of the scattered light decreased almost twice in presence of 200 nM of BSA. Addition of 20 nM PEG changed light scattering, too. This concentration of additives also increased the substrate oxidation yield. The addition of BSA and PEG to the mixture containing phenol, bisphenol A or 1-hydroxypyrene practically didn't influence the intensity of scattered light (Table 1).

To reveal the nature of scattered light, solutions containing oxidized substrates were analysed with a microparticle counter.

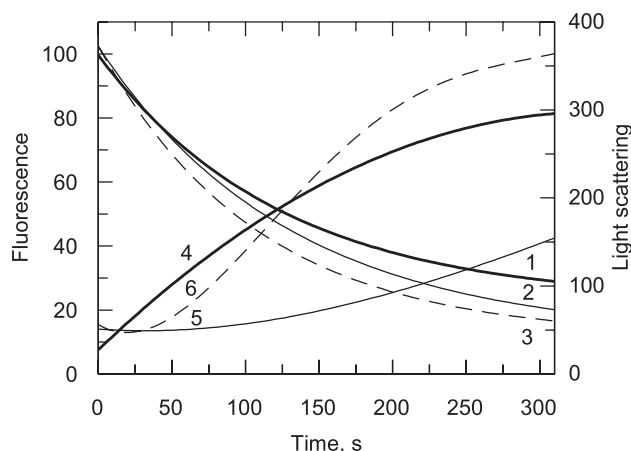


Fig. 3. Change of fluorescence (1–3) and light scattering (4–6) during the oxidation of 1-naphthol in presence of BSA (2, 5) and PEG (3, 6). Concentration of 1-naphthol 25 μM , BSA 200 nM, PEG 20 nM, rCiP 1 nM, H_2O_2 0.1 mM

During exhaustive 1-naphthol oxidation, formation of particles with the mean diameter of 8 μm was observed (Fig. 4). The amount of particles was $1.5 \cdot 10^4$ per ml (Table 2). The oxidation of 1-naphthol in presence of 20 nM PEG increased the mean diameter of particles, however, the amount of particles increased but little (up to $1.7 \cdot 10^4$ 1/ml). Nevertheless the volume of the par-

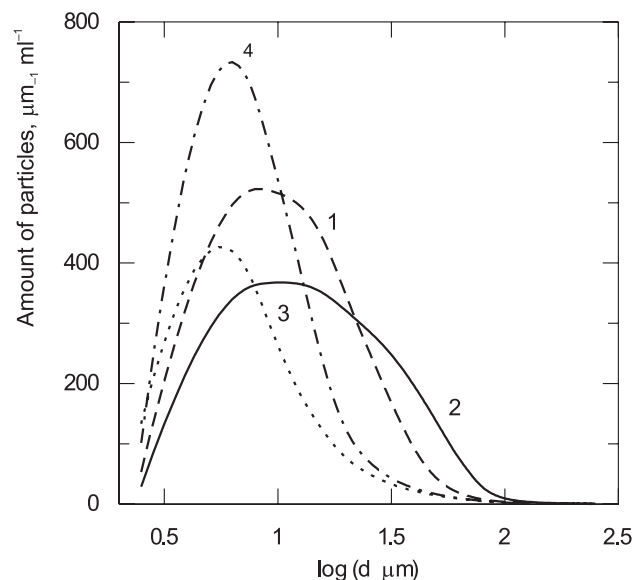


Fig. 4. Dependence of the amount of particles on diameter of particles formed during 1-naphthol (1, 2) and 4-hydroxybiphenyl (3, 4) oxidation in absence (1, 3) and presence of PEG (2, 4) at pH 5.5. Concentration of 1-naphthol 25 μM , 4-hydroxybiphenyl 10 μM , PEG 10 μM , H_2O_2 0.1 mM, rCiP 1 nM, 50 mM acetate buffer

ticles calculated from the integration of the particles within all diameters was much larger in presence of PEG, i. e. $1.1 \cdot 10^{-4}$ in its absence and $6.1 \cdot 10^{-4} \text{ cm}^3/\text{ml}$ in presence. The calculated volume was 30 and 170 times larger in comparison to the amount of the substrate, indicating that microparticles had a porous structure.

The average diameter of particles formed during 4-hydroxybiphenyl oxidation was smaller, and the amount of particles increased in presence of PEG (Fig. 4). The calculated volume of the particles was the same or 9 times larger than the substrate amount in absence or presence of PEG, respectively. A small diameter of particles and their low volume indicated that microparticles formed during 4-hydroxybiphenyl oxidation had a more compact structure.

Investigation of the dependence of 1-naphthol oxidation rate on pH showed that the conversion correlated with pH dependence on the initial rate (Fig. 5). The apparent pK_a values of activity increase and decrease was 5.6 ± 0.1 and 9.4 ± 0.1 , whereas the pK_a of conversion was 5.0 ± 0.2 and 9.8 ± 0.2 , respectively (Fig. 5). However, light scattering decreased at pH less than 6. An apparent pK_a of this process was 5.2 ± 0.9 and 7.4 ± 0.5 . These results indicate a complex nature of particle formation and enzyme activity inhibition.

Structure–activity relationship of hydroxyaryl oxidation

Experimental data show that the kinetics of HA oxidation is complicated by enzyme inhibition. Analysis of the initial rates of HA oxidations allows to avoid this difficulty. The apparent bimolecular constants of HAs obtained from the initial rate varied by three orders of magnitude (Table 1). To determine the structure–activity relationship, the HOMO, the HOMO–LUMO gap, the ratio of polar surface area (PSA) to total surface area (SA), the distribution coefficient ($\log P$), the lipole parameter and the docking energy of HAs were calculated (Table 3). All these parameters showed good correlations with HA reactivity. The squared correlation coefficient

Table 2. Amount and volume of microparticles formed during 1-naphthol and 4-hydroxybiphenyl oxidation at 25 °C in 50 mM acetate buffer, pH 5.5. Concentration of 1-naphthol 25 μM , 4-hydroxybiphenyl 10 μM , H_2O_2 0.1 mM, rCIP 1 nM, PEG 20 nM

Substrate	PEG, nM	Number of particles, 1/ml	Particles volume, cm^3/ml
1-naphthol	–	$1.5 \cdot 10^4$	$1.1 \cdot 10^{-4}$
1-naphthol	20	$1.7 \cdot 10^4$	$6.1 \cdot 10^{-4}$
4-hydroxybiphenyl	–	$6.8 \cdot 10^3$	$1.8 \cdot 10^{-6}$
4-hydroxybiphenyl	20	$1.1 \cdot 10^4$	$1.5 \cdot 10^{-5}$

Table 3. Calculated parameters of hydroxyaryls (1 a.u. = 27.2116 eV)

Hydroxyaryl	HOMO, a.u.	HOMO–LUMO gap, a.u.	PSA/SA	$\log P$	Lipole	Docking energy, kcal/mol
1-Hydroxypyrene	–0.249	0.330	0.11	4.86	2.80	–9.30
4-Hydroxybiphenyl	–0.278	0.388	0.14	3.87	2.71	–6.57
4,4'-Isopropylidene-diphenol	–0.290	0.426	0.23	5.31	1.33	–5.74
1-Naphthol	–0.277	0.387	0.14	3.25	2.54	–6.83
2-Naphthol	–0.280	0.382	0.16	3.25	2.85	–6.82
Phenol	–0.309	0.453	0.19	2.14	1.23	–5.30

(r^2) was 0.78, 0.90, 0.88, 0.80, 0.93 and 0.80 for linear dependence of $\ln(k_b) = f(\text{particular parameter})$.

The good correlations of $\ln(k_b)$ with many of molecular parameters allowed to conclude that the redox potential of the substrates, which is proportional to the energies of HOMO, HOMO–LUMO gap, as well as to lipole properties (hydrophobicity) of HAs are the main factors determining the HA reactivity.

Mechanism of peroxidase inhibition

Several schemes of peroxidase inactivation during HA oxidation may be suggested. The retarding effects of enzyme inactivation by BSA or by other uncharged water-soluble polymers indicate that the inhibition of activity is associated with the secondary process but not with the direct active centre modification by intermediates of the substrates. The quantum mechanical and docking calculations performed in [27] permitted to formulate the “molecular clothing” hypothesis. The essence of the hypothesis is the oligomers of HA formation. Docking and molecular dynamics calculations showed that these oligomers interacted with the enzyme stronger than the substrates. In contrast to the substrate, the binding of oligomers did not form productive complexes and blocked the active centre. The BSA, PEG or other uncharged polymers, which form a globular structure, interacted with oligomers and prevented enzyme inactivation. The kinetic scheme of this type enzyme inactivation was analysed in [16, 17].

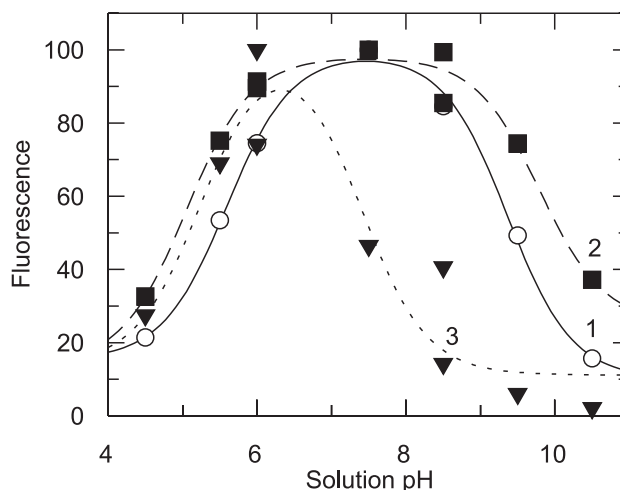


Fig. 5. The pH dependence of initial rate (1), conversion yield (2) and light scattering (3) during 1-naphthol oxidation. Concentration of 1-naphthol 25 μM , rCIP 1 nM, H_2O_2 0.1 mM. Conversion yield and light scattering were measured more than 10 min after the incubation

ACKNOWLEDGEMENTS

The research was supported by the Lithuanian State Science and Studies Foundation, project C-03020.

Received 4 January 2007

Accepted 19 February 2007

References

- Aitken MD, Chemical Engineering J. 1993; 52: B49–58.
- Klibanov AM, Alberti BN, Morris ED et al. Appl Biochem 1980; 2: 414–21.
- Alberti BN, Klibanov AM, in: Exemer JH. (ed.) Detoxification of hazardous waster. Ann. Arbor. Science, Mich., 1982; 349–56.
- Wilberg K, Assenhaimer Ch, Rubio J. Chem Technol Biotechnol 2002; 77: 851–7.
- Ikehata K, Buchanan ID. Environmental Technology 2002; 23: 1355–67.
- Ghioureliotis M, Nicell JA. Enzyme Microb Technol 1999; 25: 185–193.
- Xu FX, Koch DE, Kong IC, Hunter RP, Bhandari A. Water Reseach 2005; 39(11): 2358–68.
- Kennedy K, Alemany K, Warith M. Water SA 2002; 28: 149–58.
- Kobayashi Sh, Higashimura H. Prog Polym Sci 2003; 28: 1015–48.
- Aksu Z. Process Biochem 2005; 40: 997–1026.
- Klibanov AM, Morris ED. Enzyme Microb Technol 1980; 3: 119–22.
- Buchanan ID, Nicell JA. Chem Technol Biotechnol 1998; 72: 23–32.
- Chang HC, Holland RD, Bumpus JA et al. Chem Biol Inter 1999; 123: 197–217.
- Yimin W, Taylor E K, Nihar B et al. Enzyme Microb Technol 1998; 22: 315–22.
- Kinsley Ch, Nicell JA. Bioresourse Technol 2000; 73: 139–46.
- Kulys J, Vidziunaite R, Schneider P. Enzyme Microb Technol 2003; 32: 455–63.
- Bratkovskaja I, Vidziunaite R, Kulys J. Biochemistry (Moscow) 2004; 69: 985–92.
- Farhangrazi ShZ, Copeland BR, Nakayama T et al. Biochemistry 1994; 33: 2647–52.
- Nelson DP, Kiesow LA. Anal Biochem 1972; 17: 303–9.
- Wetlaufer DB. Adv Protein Chem 1962; 17: 303–90.
- Frisch MJ, Trucks GW, Schlegel HB, Gill PMW, Johnson BG, Robb MA, Cheeseman JR, Keith T, Petersson GA, Montgomery JA, Raghavachari K, Al-Laham MA, Zakrzewski VG, Ortiz JV, Foresman JB, Cioslowski J, Stefanov BB, Nanayakkara A, Challacombe M, Peng CY, Ayala PY, Chen W, Wong MW, Andres JL, Replogle ES, Gomperts R, Martin RL, Fox DJ, Binkley JS, Defrees DJ, Baker J, Stewart JP, Head-Gordon M, Gonzalez C, Pople JA. Gaussian 94. Revision E.1. Pittsburgh PA: Gaussian, Inc., 1995.
- Kunishima N, Fukuyama K, Matsubara H et al. Mol Biol 1994; 235: 331–4.
- Berglund GI, Carlsson GH, Smith AT et al. Nature 2002; 417: 463–8.
- Morris GM, Goodsell DS, Halliday RS et al. Comp Chem 1998; 19: 1639–62.
- Mehler EL, Solmajer T. Protein Eng 1991; 4: 903–10.
- Pedretti A, Villa L, Vistoli G, J. Mol Graph Model 2002; 21(1): 47–9.
- Ziemys A, Kulys J. Comp Biol Chem 2005; 29: 83–90.

J. Kulys, R. Vidžiūnaitė, A. Žiemys, I. Bratkovskaja

HIDROKSILARILŲ OKSIDACIJOS GRYBINE PEROKSIDAZE YPATUMAI: FERMENTO AKTYVUMAS IR INHIBICIJA

Santrauka

Tirta hidroksiarilų (HAs), t. y. fenolio, 1-naftolo, 2-naftolo, 4,4'-izopropilideno difenolio (bisfenolis A), 4-hidroksibifenilo ir 1-hidroksipireno oksidacijos, katalizuojamos rekombinantine *Coprinus cinereus* peroksidaze (rCiP), kinetika, ypač pabrėžiant substratų struktūros ir funkcijos ryšį.

Tirti HAs rodė skirtingą reaktumą. Maksimalus (HAs) oksidacijos greitis stebimas esant pH 7,0–7,5. Aktyvumo kaitos tariamosios pK_s reikšmės 1-naftolui – 5,6 ir 9,4. HAs oksidacijos tariamosios bimolekulinės konstantos (k_b) kito nuo $1,3 \cdot 10^5$ iki $1,3 \cdot 10^8 \text{ M}^{-1}\text{s}^{-1}$ esant pH 5,5 ir 25 °C.

Palyginus pradinį HAs oksidacijos greitį su apskaičiuotais molekuliniais parametrais matyti, kad greitį lemia molekulių orbitalių energija (oksidacinis-redukcinis potencialas) ir substratų hidrofobiškumas.

Pilnos HAs oksidacijos metu buvo pastebėta peroksidazės inhibicija ir mikrodalelių susidarymas. BSA ir PEG stabdė inhibiciją ir padidindavo HAs oksidacijos išeigą. Siūloma hipotezė, kad rCiP inhibicija yra susijusi su HAs oligomerų susidarymu, kurie jungiasi aktyviame peroksidazės centre. Substratų kompleksacijos aktyviame centre skaičiavimai rodo, kad šie oligomerai sąveikauja su fermentu stipriau nei substratai. Oligomerai nesudaro produktyvių kompleksų ir blokuoja aktyvų centrą. BSA, PEG ir kiti krūvio neturintys ir globulines struktūras sudarantys polimerai sujungia oligomerus ir apsaugo fermentą nuo inhibicijos.